



Synthesis and characterization of [^{125}I]2-iodo *N*-[*(S)*-{(*S*)-1-methylpiperidin-2-yl}(phenyl)methyl]3-trifluoromethyl-benzamide as novel imaging probe for glycine transporter 1

Takeshi Fuchigami^{a,b,*}, Mamoru Haratake^a, Yasuhiro Magata^b, Terushi Haradahira^c, Morio Nakayama^{a,*}

^a Graduate School of Biomedical Sciences, Nagasaki University, 1-14 Bunkyo-machi, Nagasaki 852-8521, Japan

^b Photon Medical Research Center, Hamamatsu University School of Medicine, Hamamatsu 431-3192, Japan

^c Faculty of Pharmaceutical Sciences, Nagasaki International University, 2825-7 Huis Ten Bosch, Sasebo, Nagasaki 859-3298, Japan

ARTICLE INFO

Article history:

Received 16 August 2011

Revised 6 September 2011

Accepted 7 September 2011

Available online 10 September 2011

Keywords:

Glycine transporter 1 (GlyT1)
 ^{125}I

Single photon emission computed tomography (SPECT)

Schizophrenia

ABSTRACT

In this study, 2-iodo substituted 1-methylpiperidin-2-yl benzamide derivatives were synthesized and evaluated as candidate SPECT imaging agents for glycine transporter 1 (GlyT1). In JAR cells, which predominantly express GlyT1, 2-iodo *N*-[*(S)*-{(*S*)-1-methylpiperidin-2-yl}(phenyl)methyl]3-trifluoromethyl-benzamide (**5**) showed excellent inhibitory activity of [^3H]glycine uptake ($\text{IC}_{50} = 2.4 \text{ nM}$). Saturation assay in rat cortical membranes revealed that [^{125}I]**5** had a single high affinity binding site with a K_d of 1.54 nM and a B_{max} of 3.40 pmol/mg protein. In vitro autoradiography demonstrated that [^{125}I]**5** showed consistent accumulation with GlyT1 expression. The in vitro binding was greatly inhibited by GlyT1 inhibitors but not by other site ligands, which suggested the high specific binding of [^{125}I]**5** with GlyT1. In the biodistribution and ex vivo autoradiography studies using mice, [^{125}I]**5** showed high blood-brain barrier permeability (1.68–2.17% dose/g at 15–60 min) and similar regional brain distribution pattern with in vitro results. In addition, pre-treatment of GlyT1 ligands resulted in significant decrease of [^{125}I]**5** binding in the GlyT1-rich regions. This preliminary study demonstrated that radio-iodinated **5** is a promising SPECT imaging probe for GlyT1.

© 2011 Elsevier Ltd. All rights reserved.

1. Introduction

Glycine has dual physiological functions as an inhibitory neurotransmitter for strychnine-sensitive glycine receptors (GlyRs) and as a co-agonist for NMDA receptors which play key roles in excitatory glutamatergic transmission.¹ Glycine transporters (GlyTs) modulate these neurotransmissions by controlling glycine concentration in the synaptic cleft of glial and neuronal cells. GlyTs are classified into two sodium/chloride dependent transporters, GlyT1, and GlyT2.² It is considered that GlyT2 participate in inhibitory glycinergic neurotransmission, because they are mainly expressed by glycinergic neurons in the caudal regions, such as the spinal cord and brain stem. In contrast, GlyT1 are widely expressed in many brain regions, such as the forebrain and caudal regions. Therefore GlyT1 are thought to regulate the glycine concentration in both excitatory NMDA receptors and inhibitory GlyRs.³

Dysfunction of the NMDA receptor is thought to be involved in various disorders, such as schizophrenia, stroke, Parkinson's

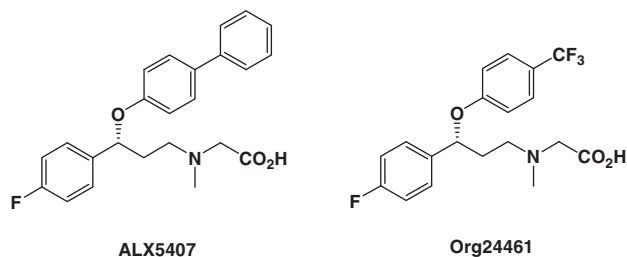
disease, and Alzheimer's disease.⁴ Alterations in the ambient glycine concentration are known to have modulatory effects on the NMDAR.³ Specifically, pharmacological modulation of glycine-mediated neurotransmission by recently developed various GlyT-1 inhibitors (Fig. 1) revealed beneficial effect to the negative and cognitive symptoms of schizophrenia.^{5–7} First generation GlyT1 inhibitors are glycine derivatives, such as ALX5407 and Org24461 with high inhibitory potency.⁸ Unfortunately, none of these compounds are expected to be promising drug candidates because of their safety profiles and pharmacokinetics.⁹ More recently, second generation nonamino acid type series of compounds have been developed as potent GlyT1 inhibitors. Some of them showed positive results for clinical use in the treatment of schizophrenia.^{6,9} In addition, recent reports suggested that GlyT1 inhibitors could be also applied for various disorders such as depression, anxiety, seizures, and neuropathic pain by modulating NMDA receptor or inhibitory GlyRs.^{10,11} However, the existence of a correlation between the progress of such diseases and the change of GlyT1 expression and activity remains to be solved.

Positron emission tomography (PET) and single photon emission computed tomography (SPECT) are the efficient imaging methods for noninvasive visualization of target proteins. Development of novel imaging probes for GlyT1 is, thus, considered useful for obtaining

* Corresponding authors. Tel./fax: +81 95 819 2443 (T.F.); tel./fax: +81 95 819 2441 (M.N.).

E-mail addresses: t-fuchi@nagasaki-u.ac.jp (T. Fuchigami), morio@nagasaki-u.ac.jp (M. Nakayama).

Amino acid type



Nonamino acid type

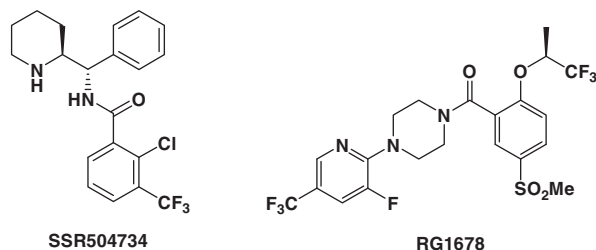


Figure 1. Chemical structure of GlyT1 selective inhibitors.

information about such diseases and occupancy of GlyT1 inhibitors in vivo. Most recently, several nonamino acid type ^{11}C or ^{18}F radiotracers were developed as PET potential ligands for GlyT1 as shown in Figure 2. The [^{18}F]MK-6577 and [^{11}C]GSK931145 had been demonstrated to be promising GlyT1 imaging agents because of good blood–brain barrier permeability, consistent accumulation with GlyT1 expression, and displacement to homogenous level by GlyT1 ligands in the pig or rhesus monkey brain in vivo.^{12,13} Furthermore [^{11}C]GSK931145 was applied for human PET studies which resulted in similar binding property with nonhuman brain. However, this tracer showed unsatisfactory signal-to-noise ratio and reproducibility because of significantly lower plasma free fraction and K_1 value in humans.¹⁴ On the other hand, SSR504734 and its derivatives have been reported that selective and competitive inhibitors of GlyT-1 recently.^{15,16} Since these compounds have molecular weight of approximately 400 and possess moderate lipophilicity, they may be useful lead compounds for the development of imaging agents. In a most recent report, SSR504734-related radioligands such as [^{11}C]SA1 showed high brain uptake and consistent accumulation with GlyT1 distribution in the monkey brain; however, the total volume of distribution (V_t) was not significantly decreased by GlyT1 ligands.¹⁷

The clinical usefulness of recently developed PET ligands remains to be investigated. The need to develop new imaging agents with optimal in vivo binding property still arises. In addition, there is still no SPECT imaging agent for GlyT1 reported. Accordingly, the aim of this study was to develop new SPECT imaging agents; wherein, a radioiodine atom was introduced into the 2-position

of SSR504734 derivatives. Hence, we present the synthesis of new GlyT1 ligands, ^{125}I labeling, and preliminary in vitro and in vivo binding characterization in rodents.

2. Results and discussion

2.1. Chemistry

The synthetic scheme of *N*-Me-SSR504734 (**4**) and 2-iodo-substituted SSR504734 derivatives (**3** and **5**) were presented in Scheme 1. (*S*)-{(*S*)-1-allylpiperidin-2-yl}(phenyl)methanamine (**1**) was prepared according to the literature.¹⁸ General coupling reaction of **1** with 3-trifluoromethyl-2-iodobenzoic acid resulted in 71% yield of amide **2**. Subsequent Pd(0) catalyzed deprotection of allyl group provided compound **3** (88% yield). Finally, reductive amination of SSR504734¹⁸ and **3** yielded 94% of *N*-Me-SSR504734 (**4**) and 95% of compound **5**.

2.2. [^3H]glycine uptake assay

Assays for the inhibitory activities of GlyT1 were performed based on the reported method utilizing [^3H]glycine uptake into JAR cells.¹⁹ The inhibitory activity of each compound was expressed as IC_{50} values as shown in Table 1. Whereas SSR504734 showed modest inhibitory activity ($\text{IC}_{50} = 80.1$ nM), its *N*-methyl derivative **4** showed 11-fold higher activity ($\text{IC}_{50} = 7.51$ nM). These results are consistent with the literature; wherein, GlyT1 expressed in CHO cells resulted in the respective IC_{50} of 314 and 2.5 nM for SSR504734 and **4**.¹⁶ Introduction of an iodine atom into the X-position of SSR504734 resulted in the improvement of inhibitory activity (**3**, 43.0 nM). Notably, compound **5** exhibited excellent inhibitory activity ($\text{IC}_{50} = 2.4$ nM), which was 18-fold and triplicate higher than **3** and **4**, respectively. These results indicate the importance of the methyl group in R-position for GlyT1 inhibition and the iodine atom is preferred over the chloride atom in the X-position to manifest strong inhibitory activity. On the other hand, a first generation GlyT1 inhibitor, ALX5407, showed sixfold higher inhibitory activity than **5** ($\text{IC}_{50} = 0.39$ nM). This extraordinary potent inhibitory activity of ALX5407 correlates with the result of a previous report ($\text{IC}_{50} = 0.3$ nM).²⁰

2.3. Radiochemistry

According to the [^3H]glycine uptake assay, this study investigated the potential of radio-iodinated **5** as a candidate SPECT imaging agent for GlyT1. Preparation of [^{125}I]**5** is shown in Scheme 2. The synthesis of [^{125}I]**5** from tributyltin precursor was initially carried out; however, radioiodination of the tributyltin precursor did not proceed. The reason was probably due to steric hindrance of the precursor (data not shown). Therefore, trimethyltin precursor **6** was prepared from compound **5** by an iodo-to-trimethyltin exchange reaction (67% yield). Then, [^{125}I]**5** was successfully synthesized by the reaction of **6** and [^{125}I]NaI (carrier-free) in the

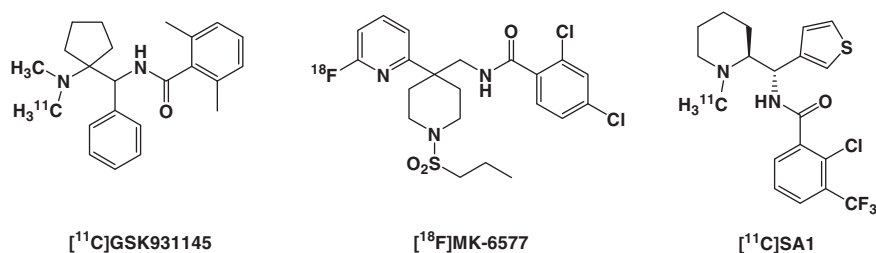
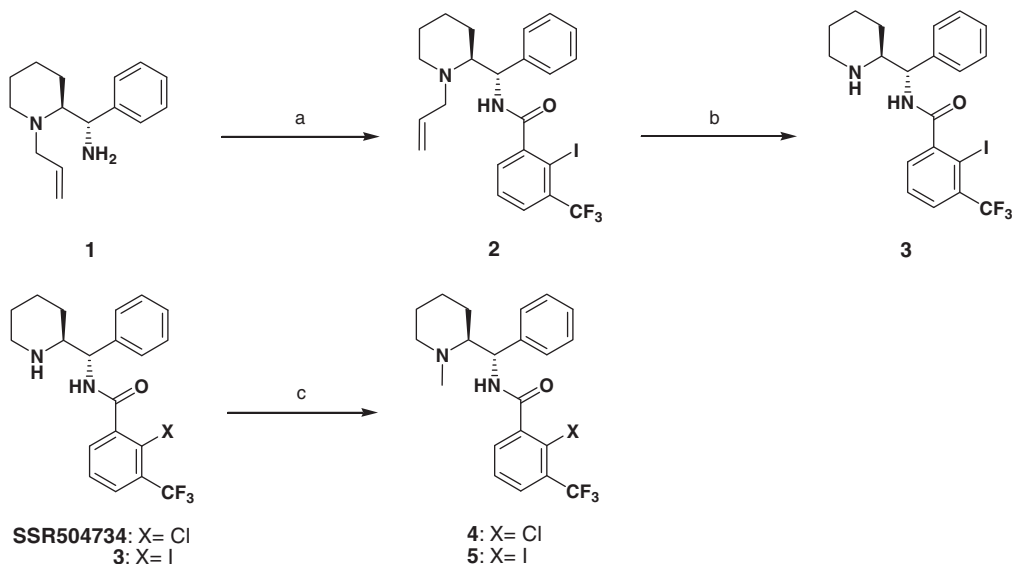


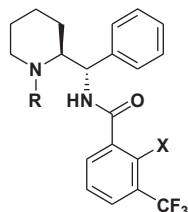
Figure 2. Chemical structure of PET probes for GlyT1.



Scheme 1. Preparation of *N*-(phenyl(piperidin-2-yl)methyl)benzamides (**4** and **5**). Reagents and conditions: (a) 3-trifluoromethyl-2-iodobenzoic acid, HOAt, EDC, triethylamine, DMF, rt, 3 h, 71%; (b) 1,3-dimethylbarbituric acid Pd(PPh₃)₄, CH₂Cl₂, 35 °C, 2 h, 88%; (c) HCHO, NaBH(OAc)₃, EtOH, rt, 6–8 h, 94% for compound **4**, 95% for compound **5**.

Table 1

IC₅₀ value of compounds calculated from inhibition assay of [³H]glycine uptake in GlyT1 expressing cells (JAR cells)



Compounds	R	X	Inhibition of [³ H]glycine uptake (IC ₅₀ , nM)	
			hGlyT1c/CHO cells ^a	JAR cells ^b
SSR504734	H	Cl	314	80.1 ± 7.55
3	H	I	2.5	43.0 ± 4.12
4	CH ₃	Cl	2.5	7.51 ± 1.91
5	CH ₃	I	2.5	2.35 ± 0.35
ALX5047				0.39 ± 0.05

^a Data from Ref. 16. The assay was inhibition study of [³H]glycine uptake to recombinant mammalian cells with stable expression of human GlyT1c (hGlyT1c/CHO cells).

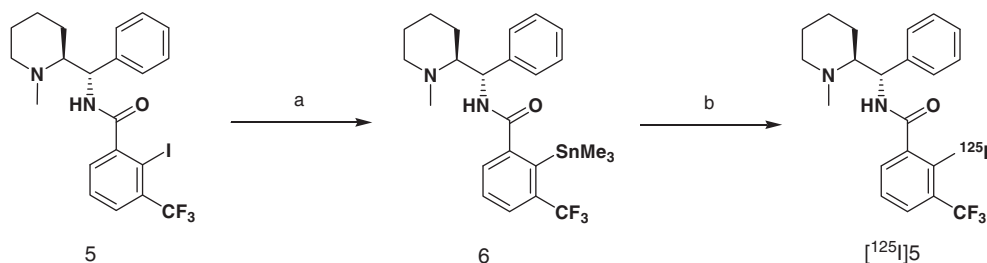
^b Inhibition assay of [³H]glycine uptake was carried out using JAR cells. IC₅₀ values are averages of at least three measurements. Values were presented as mean ± SEM.

presence of chloramine-T and HCl at 60 °C for 40 min. The radiochemical yield based on [¹²⁵I]NaI was 13–19% and the radiochemical purity was >98%.

2.4. In vitro binding characterization

In order to investigate the binding property of [¹²⁵I]**5**, saturation assays in the rat cortical brain homogenates were carried out. The saturation curve and scatchard plot are shown in Figure 3. The binding of [¹²⁵I]**5** was calculated to be a well-fitted one binding site model ($R_2 = 0.985$) with high affinity ($K_d = 1.58 \pm 0.34$ nM). The B_{max} value was estimated to be 3.40 ± 0.18 pmol/mg protein which is consistent with the results of other radioligands for GlyT1.^{21,22}

To characterize in vitro regional brain distributions of [¹²⁵I]**5**, autoradiography experiments using the rat brain sections were performed. As shown in the autoradiogram in Figure 4, [¹²⁵I]**5** showed high accumulation in the corpus callosum, thalamus, mid-brain, medullary, and cerebellar white matter. On the other hand, low uptake of [¹²⁵I]**5** was observed in the cerebral cortex, hippocampus, striatum, and cerebellar gray matter (Fig. 4A and C). It should be noted that the accumulation pattern of [¹²⁵I]**5** was quite similar to the distribution of GlyT1 immunoreactivity in the rat brain.²³ Nonspecific binding was determined in the presence of corresponding nonradioactive **5** (10 μM), which resulted in a



Scheme 2. Preparation of [¹²⁵I]**5**. Reagents and conditions: (a) (Me₃Sn)₂(Ph₃P)₄Pd, triethylamine, dioxane, 110 °C, 67%, (b) [¹²⁵I]NaI, chloramine-T, HCl, EtOH, 80 °C, 40 min, 13–19%.

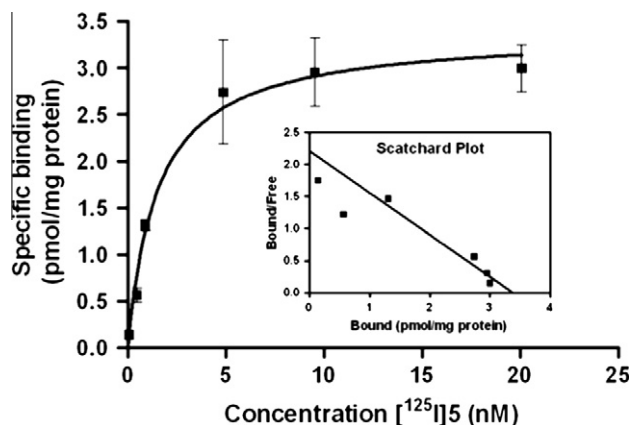


Figure 3. Saturation curve and scatchard plot of [^{125}I]5 binding to rat forebrain membranes. K_d and B_{max} values were determined by saturation analysis using increasing concentrations of [^{125}I]5 (0.1–20 nM). Nonspecific binding was determined with 10 μM of unlabeled 5.

significant reduction of radioactivity accumulation in the whole brain compared with total binding. Additionally, regional differences in the [^{125}I]5 binding disappeared in the brain regions (Fig. 4B and C). These results indicate that the specific binding of [^{125}I]5 in the rat brain slices correlates with GlyT1 expression level.

In order to investigate the specificity of [^{125}I]5 binding to GlyT1, in vitro inhibition studies were performed using GlyT1 inhibitors [SSR504734, **4** (*N*-Me-SSR504734), ALX5047, and HPCP {(+)-*N*-[cis-1-(2-Hydroxy-2-phenyl-cyclohexyl)-piperidin-4-yl]-4-methoxy-*N*-phenyl-benzenesulfonamide: potent GlyT1 inhibitor²⁴]} and a GlyT1 substrate (glycine), as well as a GlyT2 inhibitor (ORG25543) and an NMDA receptor glycine site antagonist (L-701,324) as shown in Table 2. In the presence of SSR504734 and its *N*-methyl derivative **4** (10 μM), the regional accumulation of [^{125}I]5 was dramatically decreased in the GlyT1-rich regions, such as the corpus callosum, thalamus, midbrain, medullary, and

cerebellum (21–27% and 20–29% compared with control, respectively). In contrast, a relatively lower reduction of radioactivity was observed from the GlyT1-poor regions, such as the cerebral cortex, hippocampus, and striatum (32–45% and 32–46%, respectively). HPCP, which has a different structure from [^{125}I]5, also showed strong inhibition of [^{125}I]5 binding to GlyT-rich regions (11–23% compared with control) and moderate reduction of radioactivity accumulation in GlyT1-poor regions (31–56%). Treatment with ALX5047 decreased [^{125}I]5 binding in all brain regions; however, the extent was lower than other GlyT1 inhibitors. The reason might be caused by allosteric inhibition of ALX5047 to the [^{125}I]5 binding for GlyT1. Indeed, it is reported that the SSR504734 derivatives have been identified as competitive inhibitors of GlyT1; whereas, ALX5047 exhibits a noncompetitive GlyT1 inhibitory activity.¹⁶ While 1 mM of glycine had almost no effect on the [^{125}I]5 binding, the increase to 10 mM caused reduction of accumulated radioactivity in all brain regions. These results suggest that compound **5** is a competitive inhibitor to the glycine binding site of GlyT1 and the binding affinity of glycine to the [^{125}I]5 binding site is much lower than the GlyT1 inhibitors. This binding property is similar to **4** (*N*-Me-SSR504734) as reported previously.¹⁶ ORG25543 and L-701,324 did not affect the [^{125}I]5 binding in all brain regions.

The results of in vitro experiments indicate that [^{125}I]5 selectively binds to GlyT1. Therefore, further in vivo studies were performed in order to validate the effectiveness of radio-iodinated **5** as a SPECT imaging agent for GlyT1.

2.5. In vivo studies

The biodistribution studies of [^{125}I]5 were carried out using normal mice and the results are shown in Table 3. High pulmonary uptake of [^{125}I]5 was observed at all points in time (9.34–17.19% dose/g), which could be attributed to the piperidine moiety of this tracer. Initial brain uptake of [^{125}I]5 was 0.51% dose/g at 0.5 min after intravenous injection. Radioactivity of [^{125}I]5 in the brain tissue increased with time and peaked to 2.42% dose/g at 30 min,

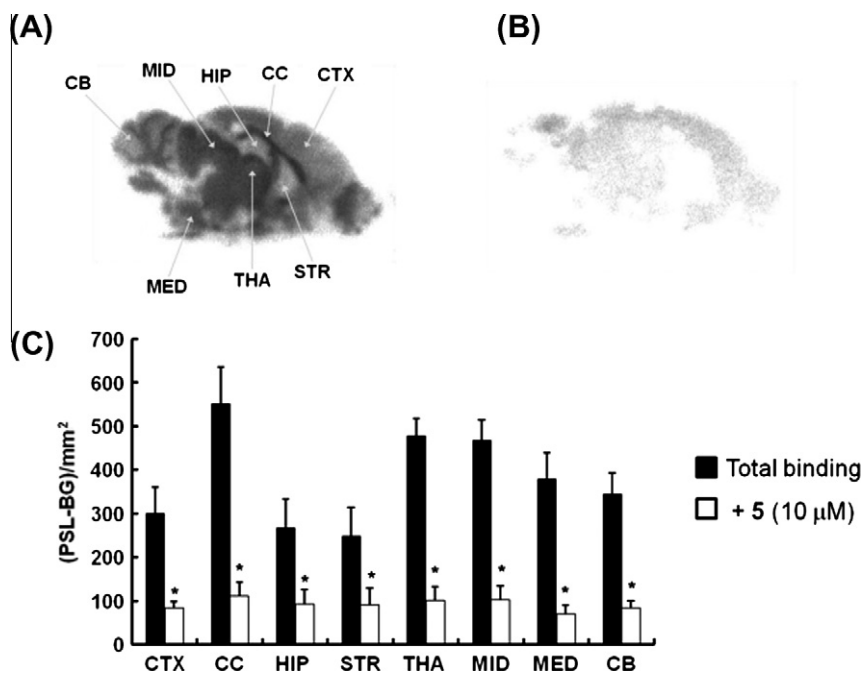


Figure 4. Autoradiograms of in vitro total binding of [^{125}I]5 (A), nonspecific binding of [^{125}I]5 (B), were visualized. The quantified values of [^{125}I]5 in the cerebral cortex (CTX), corpus callosum (CC), hippocampus (HIP), thalamus (THA), midbrain (MID), medullary (MED), and cerebellum (CB) were expressed as (PSL-BG)/mm² (mean \pm SD, $n = 4$ –5 from at least three rats). (C), Nonspecific binding was determined in the presence of corresponding nonradioactive **5** (10 μM). * $P < 0.05$ in comparison to the control group (Mann–Whitney *U*-test).

Table 2
Effects of drugs on in vitro binding of [¹²⁵I]5 to rat brain slices

Drugs	Concentration (mM)	% Control binding of [¹²⁵ I]5 ^b							
		CTX	CC	HIP	STR	THA	MID	MED	CB
GlyT1 Inhibitor									
SSR504734	0.01	29.3	21.8	46.3	50.2	29.6	28.9	31.7	27.7
4 (N-Me-SSR504734)	0.01	37.5	20.2	45.8	32.2	25.1	25.3	20.6	28.9
HPCP ^a	0.01	31.0	19.7	55.9	31.8	22.5	19.7	20.5	23.0
ALX5407	0.01	57.6	27.8	63.2	46.7	33.2	36.2	25.3	43.1
Substrate									
Glycine	1	89.6	94.1	107.6	121.5	107.6	105.8	104.1	97.4
	10	43.7	39.6	71.5	47.6	52.7	52.1	61.2	44.9
GlyT2									
ORG25543	0.01	95.1	98.2	104.9	103.6	99.7	115.0	91.4	123.8
NMDA receptor glycine site									
L-701324	0.01	92.5	92.5	90.9	96.8	87.1	81.3	104.1	87.1

^a HPCP; (+)-N-[cis-1-(2-Hydroxy-2-phenyl-cyclohexyl)-piperidin-4-yl]-4-methoxy-N-phenyl-benzenesulfonamide.²⁴^b % Contro binding was calculated from average values obtained by at least triplicate slices from three rats.**Table 3**
Biodistribution data for [¹²⁵I]5 in normal ddY mice^a

Organ	0.5 min	5 min	15 min	30 min	60 min	180 min
Blood	1.35 ± 0.37	0.87 ± 0.22	0.69 ± 0.09	0.90 ± 0.17	0.80 ± 0.09	0.85 ± 0.15
Liver	1.82 ± 0.62	9.25 ± 1.98	11.51 ± 1.85	14.74 ± 1.93	16.04 ± 1.53	15.05 ± 3.49
Kidney	4.05 ± 1.14	10.71 ± 2.20	8.86 ± 1.96	10.22 ± 1.00	8.27 ± 0.50	6.97 ± 1.73
Intestine	0.81 ± 0.24	2.47 ± 0.60	3.25 ± 0.64	5.76 ± 1.21	9.59 ± 1.06	17.13 ± 1.82
Spleen	0.97 ± 0.25	5.11 ± 1.27	5.50 ± 0.68	7.68 ± 1.59	5.86 ± 1.17	3.41 ± 1.15
Lung	17.19 ± 3.91	19.30 ± 4.14	15.24 ± 2.03	17.07 ± 3.03	12.09 ± 2.47	9.34 ± 3.82
Stomach	0.83 ± 0.33	3.30 ± 0.73	5.22 ± 1.81	8.66 ± 1.75	8.26 ± 2.97	12.73 ± 4.64
Pancreas	1.18 ± 0.43	6.40 ± 1.60	7.93 ± 1.42	12.02 ± 1.09	9.51 ± 1.13	4.84 ± 1.21
Heart	8.19 ± 1.58	5.17 ± 0.59	3.38 ± 0.59	3.95 ± 0.45	2.79 ± 0.30	1.79 ± 0.38
Brain	0.51 ± 0.16	1.33 ± 0.15	1.68 ± 0.30	2.17 ± 0.40	1.85 ± 0.21	0.73 ± 0.23
Brain to blood	0.38 ± 0.05	1.57 ± 0.25	2.42 ± 0.18	2.46 ± 0.41	2.32 ± 0.12	0.85 ± 0.15

^a [¹²⁵I]5 (11.1 kBq) was injected intravenously via tail vein into ddY mice (Male, 6 W, 30–35 g). Values were presented as mean ± SD (% dose/g, n = 5–6).

suggesting the good blood–brain barrier permeability of [¹²⁵I]5. Although brain uptake of [¹²⁵I]5 gradually decreased after 30 min, brain to blood ratios remained at the same level at 60 min (2.46% and 2.32% dose/g at 30 and 60 min, respectively). It is suggested that radiotracers with moderate lipophilicity (log_{D7,4} values; 2.0–3.5) show optimal passive brain entry under in vivo condition.^{25,26} Indeed, the experimental log_{D7,4} value of [¹²⁵I]5 was 2.86 (data not shown); therefore, high brain uptake of [¹²⁵I]5 can be partially explained in terms of ideal lipophilicity of [¹²⁵I]5. Metabolisms of [¹²⁵I]5 in the mice brain were analyzed by radio-TLC of brain homogenates obtained at 5, 30, and 60 min post-injection; and 92%, 90%, and 89%, respectively, of the parent compounds remained unchanged (data not shown). Thus, metabolism should have little or no influence on the in vivo brain distribution pattern of [¹²⁵I]5.

Next, the specificity of regional brain binding of [¹²⁵I]5 toward GlyT1 was studied by blocking studies using nonradioactive **5**, compound **4**, SSR504734, and ALX5407 (2 mg/kg, intravenously), which were administered 15 min prior to injection of the radioligand. Because brain/blood ratio of [¹²⁵I]5 peaked at 30 and 60 min as shown in Table 3, regional brain distribution studies were conducted at 30 and 60 min after the radiotracer injection. The results of in vivo blocking studies are shown in Figure 5. Pre-injection of nonradioactive **5** resulted in significant reduction of [¹²⁵I]5 accumulation in the GlyT1-rich regions, such as the thalamus (45% and 58% compared with control at 30 and 60 min, respectively), midbrain (48% and 51%), and medullary (53% and 52%). In contrast, the extent of reduction of [¹²⁵I]5 uptake in the GlyT1-poor regions, such as the hippocampus and striatum was

relatively lower than the GlyT1-rich regions (Fig. 5A and C). Pre-administration of **4** also caused a significant decrease of regional radioactivity uptake in the thalamus (56% and 56% compared with control at 30 and 60 min, respectively), midbrain (55% and 48%), and medullary (59% and 47%); whereas, little displacement of radioactivity from the hippocampus and striatum was observed as shown in Figure 5A and C. The estimated brain regions to blood ratios were also significantly decreased by nonradioactive **5** and compound **4** in the brain regions with high GlyT1 density at 30 and 60 min (Fig. 5B and D). The radioactivity level of [¹²⁵I]5 in all brain regions became homogenous by these blockers both at 30 and 60 min in agreement with the in vitro autoradiography experiments. These results indicate that in vivo binding of [¹²⁵I]5 is specifically mediated by GlyT1. When SSR504734 was administered as pretreatment, the uptake of [¹²⁵I]5 reduced slightly but the change was not significant in all brain regions both at 30 and 60 min (Fig. 5A and C), in which the reason could be due to the much lower inhibitory activity (Table 1) and binding affinity¹⁶ for GlyT1 of SSR504734 than its N-methyl analogs, compounds **4** and **5**. Pretreatment with ALX5407 showed almost no effect to the regional brain uptake of [¹²⁵I]5 at 30 min. On the other hand, the brain uptake of [¹²⁵I]5 was decreased at 60 min; however, the reduction was not significant in most regions. The slow and weak inhibitory effects of ALX5407 for [¹²⁵I]5 binding agree with in vitro results (Table 2).

To investigate further in vivo binding property of [¹²⁵I]5 to GlyT1, we performed ex vivo autoradiography studies. Mice were injected intravenously with [¹²⁵I]5 and sacrificed 60 min after administration. As shown in Figure 6, a high uptake of [¹²⁵I]5

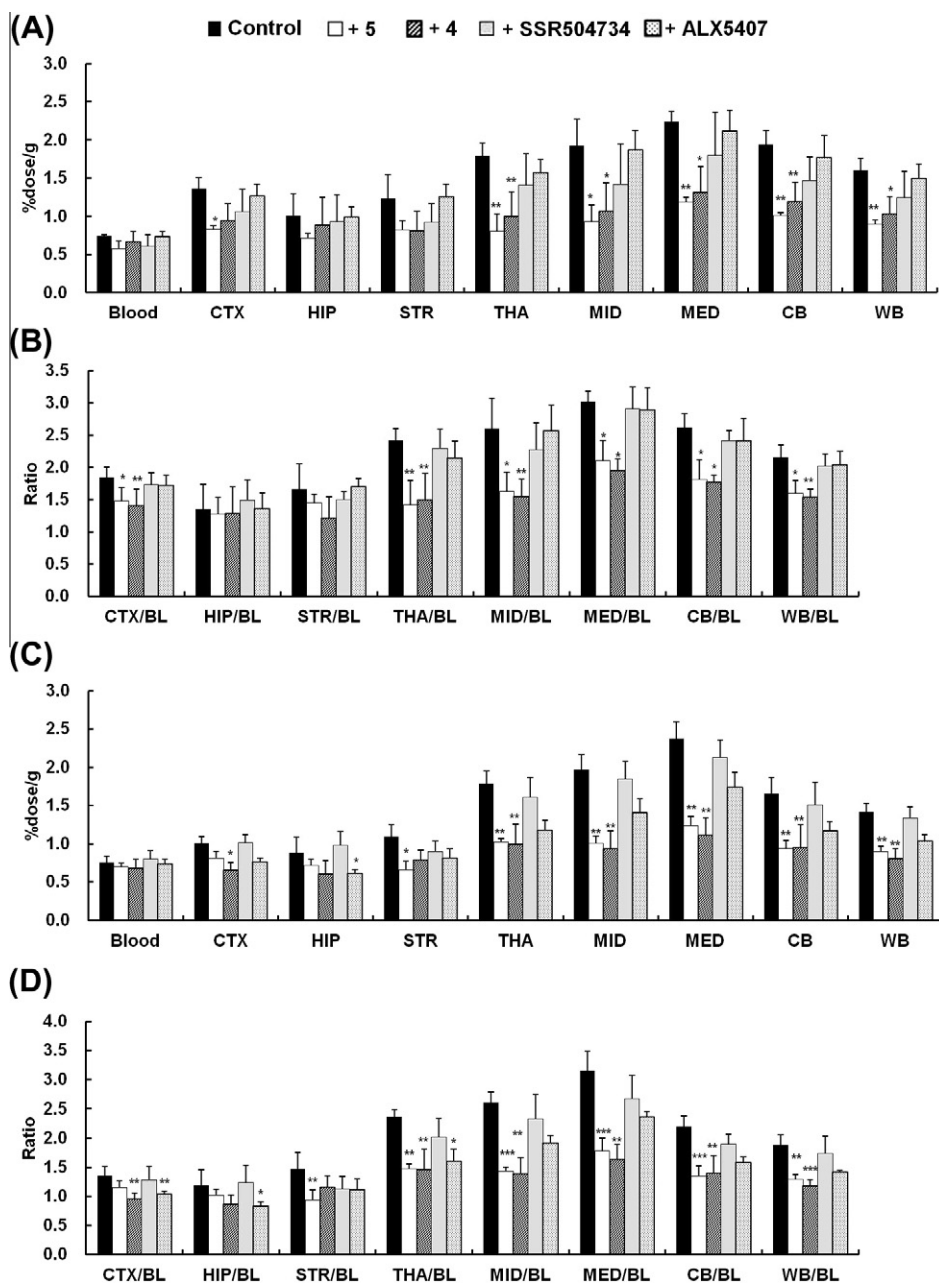


Figure 5. Effects of nonradioactive **5**, **4** (*N*-Me-SSR504734), SSR504734, and ALX504734 of [125 I]**5** in mice at 30 or 60 min after injection. Drugs (2 mg/kg) were given as pretreatment by intravenous injection 15 min before [125 I]**5** (33.3 kBq) administration. Figure 4A and B represent the percentage of the injected dose per gram of tissue (% dose/g) and organ to blood ratio of % dose/g at 30 min after injection, respectively. Figure 4C and D represent % dose/g and organ to blood ratio at 60 min after injection, respectively. Values were presented as mean \pm SD (% dose/g, $n = 5$ –6). WB represents whole brain. * $P < 0.05$, ** $P < 0.01$, *** $P < 0.001$ in comparison to the control group (Kruskal–Wallis test, post-test was Dunn's test).

was clearly visualized in the GlyT1-rich regions (thalamus, mid-brain, cerebellum, and medullary). On the other hand, the accumulation was low in the GlyT1-poor regions (cerebral cortex, hippocampus, and striatum). The low radioactivity of [125 I]**5** in the corpus callosum was inconsistent with that shown in the *in vitro* autoradiography studies. The *in vivo* results might be due to the influence of regional blood flow in the brain. It is well known that blood flow in the white matter, such as the corpus callosum was lower than that of other brain regions.^{27,28} To further confirm the *in vivo* specificity of [125 I]**5** for GlyT1, blocking studies were performed in which nonradioactive **5** or compound **4** (2 mg/kg body weight) was given as pretreatment before [125 I]**5** injection. As shown in the autoradiogram images in Figure 6B and C, both **5**

and **4** abolished the heterogenous distribution of [125 I]**5** in the brain regions. Quantified accumulation of [125 I]**5** was significantly reduced by these compounds only in the GlyT1-rich regions (Fig. 6D). These results strongly suggest that [125 I]**5** could recognize GlyT1 protein under *in vivo* conditions.

Since the accumulation of [125 I]**5** was dependent on GlyT1 expression and specific binding to GlyT1, this tracer is expected to be a promising SPECT probe for targeting GlyT1 in the living brain. Additionally, the *N*-methyl group of **5** could be labeled with carbon-11; therefore, compound **5** could be employed as a PET ligand. Further *in vivo* imaging studies of radio-labeled **5** are necessary to clarify the potential of this compound as a clinical useful imaging probe for GlyT1.

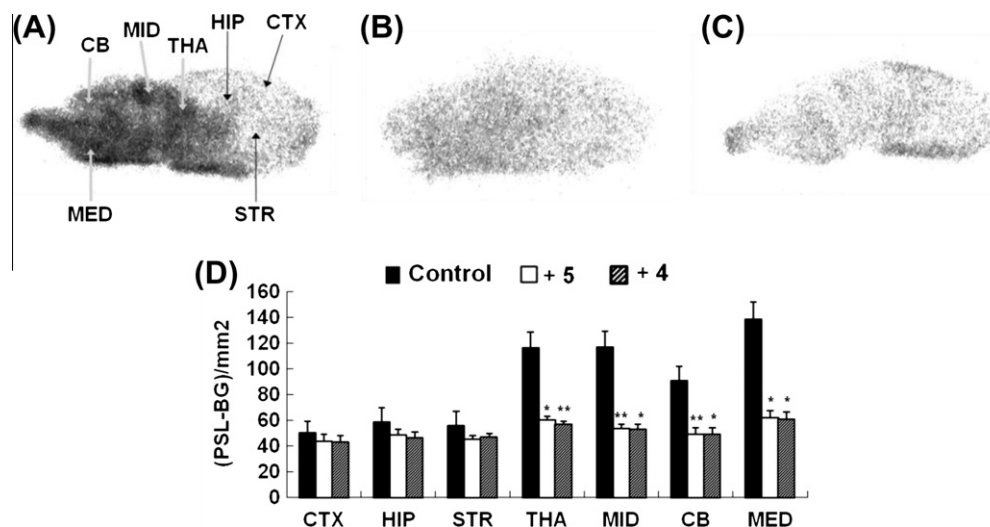


Figure 6. Ex vivo autoradiograms of [¹²⁵I]5 in the sagittal sections of mouse brains at 60 min after injection (200 kBq). In the blocking studies, drugs (2 mg/kg) were given as pre-treatment by intravenous injection 15 min before the tracer administration. (A) control [¹²⁵I]5 binding; (B) [¹²⁵I]5+ nonradioactive 5; (C) [¹²⁵I]5 + 4; (D) the quantified radioactivity of [¹²⁵I]5 in the brain regions. The radioactivity level in each region was determined from the brain images (n = 5) and was expressed by as photostimulated-luminescence (PSL)/mm² region. *P < 0.05, **P < 0.01, in comparison to the control group (Kruskal–Wallis test, post-test was Dunn's test).

3. Conclusion

In this study, [¹²⁵I]5 was developed as a candidate SPECT ligand for GlyT1. Compound 5 was discovered to possess potent GlyT1 inhibitory activity. In addition, [¹²⁵I]5 showed consistent binding with GlyT1 expression in the rodent brain and the accumulated radioactivity was significantly decreased by GlyT1 inhibitors in the GlyT1-rich regions both in vitro and in vivo. Altogether, the radio-iodinated 5 could be a promising SPECT probe for neuroimaging of central GlyT1.

4. Experimental

4.1. General information

All reagents were commercially available products and were used without further purification unless otherwise indicated. ¹H NMR spectra were obtained on a Varian Gemini 300 spectrometer with TMS as internal standard. Mass spectra were obtained on JEOL IMS-DX or JMS-T100TD instruments. HPLC analysis was performed on a Shimadzu HPLC system (LC-20AT pump with a SPD-20A UV detector, λ = 254 nm). An automated gamma counter with a NaI(Tl) detector (PerkinElmer, 2470 WIZARD²) was used to measure radioactivity.

(+)-N-[cis-1-(2-Hydroxy-2-phenyl-cyclohexyl)-piperidin-4-yl]-4-methoxy-N-phenyl-benzenesulfonamide (HPCP) was prepared according to the literature.²⁴ ORG 25543 {4-Benzyloxy-N-[1-(dimethylamino)cyclopentylmethyl]-3,5-dimethoxybenzamide} was synthesized based on a reported procedure.²⁹ [³H]glycine was purchased from Morarek Biochemicals (Brea, CA, USA). [¹²⁵I]NaI was obtained by MP biomedical (Costa Mesa, CA, USA).

The experiments with animals were conducted in accordance with our institutional guidelines and were approved by Nagasaki University Animal Care Committee. All animals were supplied by Tagawa Experimental Animal Laboratory (Nagasaki, Japan).

4.1.1. N-[(S)-{(S)-1-allylpiperidin-2-yl}(phenyl)methyl]-2-iodo-3-trifluoromethyl-benzamide (2)

2-Iodo-3-trifluoromethylacetic acid³⁰ (228 mg, 0.72 mmol) in DMF (2.5 mL) was mixed with EDC (138 mg, 0.72 mmol) and 1-hydroxy-7-azabenzotriazole (97 mg, 0.72 mmol), then stirred at

room temperature for 30 min. To this mixture, a solution of 1¹⁸ (127 mg, 0.55 mmol) and triethylamine 430 (199 μl, 1.43 mmol) in DMF (2.5 mL) was added and stirred further for 3 h. The reaction mixture was added aqueous NaHCO₃ and ethyl acetate. The organic layer was separated and washed by brine, dried with Na₂SO₄, and evaporated to dryness. The crude product was chromatographed on silica gel with hexane/EtOAc = 1:2 to provide 2 (205 mg, 0.388 mmol, 71%) as a white solid. ¹H NMR (300 MHz CDCl₃) δ 7.67 (d, J = 7.6 Hz, 1H), 7.48 (t, J = 7.4 Hz, 1H), 7.42–7.28 (m, 6H), 5.78–5.65 (m, 1H), 5.12 (d, J = Hz, 16.8 Hz), 5.09 (d, J = Hz, 9.3 Hz), 4.96 (d, J = 6.6 Hz, 9.3 Hz), 3.33–3.18 (m, 2H), 3.05–2.98 (m, 1H), 2.87–2.79 (m, 1H), 2.62–2.53 (m, 1H), 1.85–1.73 (m, 1H), 1.56–1.28 (m, 5H), [α]_D²⁰ = +16.2 (c = 1.0; CHCl₃), MS (FAB) m/z: 529 (M⁺).

4.1.2. 2-Iodo-N-[(S)-{(S)-1-piperidin-2-yl}(phenyl)methyl]-3-trifluoromethyl-benzamide (3)

To the stirred solution of compound 2 (172 mg, 0.33 mmol) in CH₂Cl₂ (5 mL), 1,3-dimethylbarbituric acid (153 mg, 0.98 mmol) and Pd(PPh₃)₄ (19.2 mg, 0.017 mmol) were added at room temperature. The reaction mixture was stirred for 2 h followed by quenching with saturated NaHCO₃ solution, extracted with CH₂Cl₂, washed by brine, dried with Na₂SO₄, and evaporated to dryness. The crude product was chromatographed on silica gel with CHCl₃/MeOH = 10:1 to provide 3 (142 mg, 0.29 mmol, 88%) as a white solid. ¹H NMR (300 MHz CDCl₃) δ 7.68 (dd, J = 7.0, 2.3 Hz, 1H), 7.53–7.47 (m, 2H), 7.43–7.35 (m, 4H), 7.34–7.30 (m, 1H), 5.16 (dd, J = 7.5, 3.4 Hz, 1H), 3.00 (d, J = 11.0 Hz, 1H), 2.58–2.45 (m, 1H), 2.11–1.85 (m, 6H), 1.84–1.52 (m, 2H), 1.48–1.25 (m, 2H), [α]_D²³ = +61.9 (c = 0.75; CH₃OH), HRMS (FAB) m/z: calcd for C₂₀H₂₁F₃N₂O (M⁺) 489.0651, found 489.0660.

4.1.3. 2-Chloro-N-[(S)-{(S)-1-methylpiperidin-2-yl}(phenyl)methyl]-3-trifluoromethyl-benzamide (4)

To the stirred solution of SSR504734¹⁸ (26 mg, 0.070 mmol) in CH₃CN (1 mL), 37% formaldehyde solution (19 μl, 0.246 mmol) and NaBH(OAc)₃ (60 mg, 0.281 mmol) were added and the reaction mixture was stirred for 3 h at room temperature. The mixture was added with water and extracted with CHCl₃. The organic layer was washed by brine, dried with Na₂SO₄, and evaporated to dryness. The crude product was chromatographed on silica gel with

CHCl₃/MeOH = 10:1 to provide **4** (29 mg, 0.065 mmol, 94%) as a white solid. ¹H NMR (300 MHz CDCl₃) δ 9.29 (s, 1H), 7.73 (d, *J* = 7.6 Hz, 1H), 7.65 (d, *J* = 6.6 Hz, 1H), 7.48–7.27 (m, 6H), 5.12 (dd, *J* = 9.4, 8.7 Hz, 1H), 3.72–3.58 (m, 3H), 3.20–3.15 (m, 2H), 2.75 (s, 3H), 1.87–1.67 (m, 2H), 1.66–1.52 (m, 1H), 1.44–1.30 (m, 1H), [α]_D²³ = +46.8 (*c* = 1.0; CH₃OH). HRMS (FAB) *m/z* calcd for C₂₁H₂₃ClF₃N₂O (M⁺) 411.1451, found 411.1482.

4.1.4. 2-Iodo *N*-[(*S*)-1-methylpiperidin-2-yl](phenyl)-methyl-3-trifluoromethyl-benzamide (**5**)

Using the above procedure for **4** starting from compound **3**, the title compound **5** (75 mg, 95%) was obtained as a white solid. ¹H NMR (300 MHz CDCl₃) δ 9.14 (s, 1H), 7.65 (t, *J* = 5.0 Hz, 1H), 7.51–7.47 (m, 2H), 7.43–7.30 (m, 5H), 5.10 (dd, *J* = 9.1, 8.0 Hz), 3.71–3.49 (m, 1H), 3.28–3.06 (m, 2H), 2.78 (s, 3H), 1.87–1.74 (m, 2H), 1.64–1.27 (m, 4H), [α]_D²³ = + 50.4 (*c* = 1.0; CH₃OH). HRMS (FAB) *m/z* calcd for C₂₁H₂₃F₃N₂O (M⁺) 503.0807, found 503.0819.

4.1.5. *N*-[(*S*)-1-Methylpiperidin-2-yl](phenyl)methyl-3-trifluoromethyl-2-trimethylstannyl-benzamide (**6**)

A mixture of **5** (6.0 mg, 0.012 mmol), bis(trimethyltin) (13 μl, 0.060 mmol) and Pd(PPh₃)₄ (0.7 mg, 0.595 μmol) in a mixed solvent (1.5 mL, 2:1 dioxane/triethylamine mixture) was stirred for 4 h under reflux. The solvent was removed, and the residue was purified by silica gel chromatography CHCl₃/MeOH = 10:1, which gave **6** (4.4 mg, 0.008 mmol, 67%) as a colorless oil.

¹H NMR (300 MHz CDCl₃) δ 8.97 (s, 1H), 8.28 (d, *J* = 7.4 Hz, 1H), 7.52–7.46 (m, 3H), 7.39–7.29 (m, 3H), 5.12 (d, *J* = 7.4 Hz, 1H), 3.81–3.70 (m, 1H), 3.67–3.63 (m, 1H), 3.48–3.30 (m, 3H), 2.78 (s, 3H), 1.97–1.51 (m, 2H), 1.53–1.26 (m, 2H), [α]_D²³ = +10.5 (*c* = 0.4; CHCl₃), MS (DART) *m/z* 541.09 (M⁺).

4.2. Radiosynthesis of [¹²⁵I]**5**

An aqueous solution of chloramine-T (20 μl, 15 mg/mL) was added to a mixture of [¹²⁵I] NaI (5–10 μl, 18.5–37.0 MBq, carrier-free), 1 M HCl (50 μl), and trimethylstannyl precursor **6** (0.2 mg in 100 μl of ethanol) in a sealed vial. The mixture was heated to 60 °C for 40 min and then quenched with 10% aqueous sodium bisulfite (100 μl) and saturated NaHCO₃ (500 μl). The mixture was extracted with EtOAc (500 μl × 3) was added to the mixture and dried under N₂ gas. The crude products were purified by HPLC (column; Nacalai Cosmosil 5C18-AR II, 4.6 × 250 mm, mobile phase; CH₃CN/0.1% TFA in H₂O = 35:65, flow rate: 1.0 mL/min). Radiochemical purity was assayed to be >98% by HPLC. The radiochemical yields based on [¹²⁵I] NaI were 13–19%.

4.3. [³H]glycine uptake assay

[³H]Glycine uptake assay was carried out according to the method in the literature¹⁹ with minor modification.

Human placental choriocarcinoma cells (ATCC No. HTB-144) were obtained from the American Type Culture Collection. JAR cells were cultured in six-well plates in RPMI 1640 medium containing 10% fetal bovine serum. Cells were plated at a density of 4.0 × 10⁵ cells/well and grown at 37 °C in a humidified atmosphere of 5% CO₂ for 48–60 h.

The culture medium was removed from the six-well plates and the JAR cells were incubated with 1.0 mL of TB1A buffer (120 mM NaCl, 2 mM KCl, 1 mM CaCl₂, 1 mM MgCl₂, 10 mM HEPES, 5 mM L-alanine, pH 7.5 adjusted with 1 M Tris base) with or without drugs for 1 min. Then, 1.0 mL of [³H]glycine (96.2 kBq, 4.8 GBq/mmol) in TB1A buffer was added to each well to give a final concentration of 10 μM. Nonspecific uptake was defined by the addition of unlabeled glycine at 10 mM. After incubation at room temperature for 2 h, the incubation medium was removed and rinsed with

ice-cooled TB1A buffer (2.0 mL × 2). The cells were then solubilized with 1.0 mL of 0.5 M NaOH solution and placed at room temperature overnight. Radioactivity in the cells was measured by liquid scintillation counting.

4.4. In vitro saturation assays

The in vitro saturation assays of [¹²⁵I]**5** to rat cortical membrane homogenates were performed according to the method in the literature.²¹ In brief, well washed membranes (25 μg protein) were incubated with [¹²⁵I]**5** (0.1–20 nM) in 250 μl of TB1 buffer (120 mM NaCl, 2 mM KCl, 1 mM CaCl₂, 1 mM MgCl₂, 10 mM HEPES, pH 7.5) for 60 min at room temperature. Nonspecific binding was defined by the addition of unlabeled **5** at 10 μM. Bound ligands were collected by rapid filtration using a Brandel cell harvester onto glass fiber filter (GF/B). The filters were washed rapidly three times with 2.5 mL of ice-cold assay buffer. The radioactivity of filters was measured by automated gamma counter.

4.5. In vitro autoradiography

In vitro autoradiography studies were carried out according to the previous reports.³¹ The brain sagittal sections (20 μm) were pre-incubated for 20 min at 25 °C in binding buffer (120 mM NaCl, 2 mM KCl, 1 mM MgCl₂, 1 mM CaCl₂, and 50 mM Tris-HCl, pH 7.5). These were subsequently incubated in the same buffer containing [¹²⁵I]**5** (100 kBq, 0.03–0.04 nM) at 25 °C for 30 min. The slices were rinsed triplicate for 3 min each with cold (5 °C) in washing buffer (120 mM NaCl, 50 mM Tris-HCl, pH 7.5), and subsequently dipped into cold water. The sections were dried under cold air and placed in contact with [¹²⁵I]-sensitive imaging plates (BAS-SR 2040; Fuji Photo, Film, Tokyo, Japan) for 3 days. Distributions of radioactivity on the plates were analyzed by Bio-Image Analyzer (FLA-5100; Fuji Photo, Film, Tokyo, Japan), which were photographically visualized as shown in Figure 4. Regions of interest (ROIs) on the slices were placed on the cerebral cortex, hippocampus, striatum, thalamus, midbrain, medullary, and cerebellum. The radioactivities in these regions were expressed as photostimulated luminescence (PSL) values on ROI-background PSL value per square millimeter. The specific binding was determined as the difference between total binding and binding in the presence of the corresponding nonradioactive **5** (10 μM). Selectivity studies were performed as similar procedure in the presence of several drugs (10 μM) except for glycine (1 or 10 mM).

4.6. In vivo experiments

The [¹²⁵I]**5** (0.1 mL, ca. 11.1 kBq for whole body distribution studies, ca. 33.3 kBq for regional brain distribution studies) was injected intravenously via the tail vein into ddY mice (male, 6 W, 30–35 g). At the designated time intervals, the mice were killed and the organs were dissected. The brain was further divided into the cerebral cortex, corpus callosum, hippocampus, thalamus, midbrain, medullary, and cerebellum.

The tissues were then weighed and the radioactivity was measured by automated gamma counting. Data were calculated as the percentage of the injected dose per gram of tissue (% dose/g). To assess the in vivo specific binding of [¹²⁵I]**5**, the nonradioactive **5** or GlyT1 antagonists SSR504734, **4**(*N*-Me-SSR504734), and ALX5407 (2 mg/kg in 30% DMSO/saline) were given as pre-treatment by intravenous injection 15 min before [¹²⁵I]**5** administration. Mice were killed 30 or 60 min after injection.

For ex vivo autoradiography studies, mice were injected intravenously with 200 kBq of [¹²⁵I]**5** and were sacrificed 60 min post-injection. For the inhibition experiment, nonradioactive **5** or **4** (2 mg/kg) was injected by intravenous injection 15 min before [¹²⁵I]**5** administration. The whole brain was quickly removed and

frozen on powdered dry ice. Brain sagittal sections (20 μm) were cut on a cryostat microtome. The sections were then exposed to a BAS SR2040 imaging plate for 7 days and analyzed with a phosphor imager (FLA-5100, Fujifilm).

To assess the metabolism of [^{125}I]5 in the mouse brain, the mice were killed 5, 30, and 60 min after [^{125}I]5 (185 kBq) injection, respectively. Whole brains were quickly removed, homogenized with ice-cooled MeOH (1.0 mL), and centrifuged at 3000 rpm for 10 min at 4 °C. The metabolites in MeOH extract were analyzed by radio-TLC using $\text{CHCl}_3/\text{MeOH} = 9:1$ and $\text{EtOAc}/\text{EtOH} = 1:1$ as mobile phases.

4.7. Data analysis

IC_{50} values of compounds in the [^3H]Glycine uptake assay as well as K_d and B_{max} values of [^{125}I]5 in the in vitro saturation assay were calculated by GraphPad Prism 4.0 (GraphPad Software, San Diego, CA). Statistical analysis was also performed by the GraphPad software. In vitro experiments of [^{125}I]5 presented in Figure 4 were statistically analyzed by Mann–Whitney U-test. In vivo experiments and ex vivo autoradiography of [^{125}I]5 described in Figures 5 and 6 were analyzed by the Kruskal–Wallis test with Dunn's multiple comparison post-test. A value of $P < 0.05$ was considered statistically significant.

Acknowledgments

The authors gratefully acknowledge our colleagues, Nobuya Kobashi, Ayaka Ogawa, and Yuki Yamashita for their technical help in the animal experiments. This work was supported by Grants from the Ichiro Kanehara Foundation and partially by Grant-in-Aid for Young Scientists (B) (21791180) from Japan Society for the Promotion of Science (JSPS).

References and notes

- Betz, H.; Laube, B. *J. Neurochem.* **2006**, *97*, 1600.
- Zafra, F.; Giménez, C. *IUBMB Life* **2008**, *60*, 810.
- Eulenburg, V.; Gomez, J. *Brain Res. Rev.* **2010**, *63*, 103.
- Javitt, D. C. *Mol. Psychiatry* **2004**, *9*, 984.
- Hashimoto, K. *Recent Pat. CNS Drug Disc.* **2006**, *1*, 43.
- Hashimoto, K. *Curr. Pharm. Des.* **2011**, *17*, 112.
- Bridges, T. M.; Williams, R.; Lindsley, C. W. *Curr. Opin. Mol. Ther.* **2008**, *10*, 591.
- Harsing, L. G., Jr.; Gacsalyi, I.; Szabo, G.; Schmidt, E.; Sziray, N.; Sebban, C.; Tesolin-Decros, B.; Matyus, P.; Egyed, A.; Spedding, M.; Levay, G. *Pharmacol. Biochem. Behav.* **2003**, *74*, 811.
- Harsing, L. G., Jr.; Juranyi, Z.; Gacsalyi, I.; Tapolicsanyi, P.; Czompa, A.; Matyus, P. *Curr. Med. Chem.* **2006**, *13*, 1017.
- Dohi, T.; Morita, K.; Kitayama, T.; Motoyama, N.; Morioka, N. *Pharmacol. Ther.* **2009**, *123*, 54.
- Möhler, H.; Boison, D.; Singer, P.; Feldon, J.; Pauly-Evers, M.; Yee, B. K. *Biochem. Pharmacol.* **2011**, *81*, 1065.
- Passchier, J.; Gentile, G.; Porter, R.; Herdon, H.; Salinas, C.; Jakobsen, S.; Audrain, H.; Laruelle, M.; Gunn, R. N. *Synapse* **2010**, *64*, 542.
- Hamill, T. G.; Eng, W.; Jennings, A.; Lewis, R.; Thomas, S.; Wood, S.; Street, L.; Wisnoski, D.; Wolkenberg, S.; Lindsley, C.; Sanabria-Bohórquez, S. M.; Patel, S.; Riffel, K.; Ryan, C.; Cook, J.; Sur, C.; Burns, H. D.; Hargreaves, R. *Synapse* **2011**, *65*, 261.
- Gunn, R. N.; Murthy, V.; Catafau, A. M.; Searle, G.; Bullich, S.; Slifstein, M.; Ouellet, D.; Zamuner, S.; Herance, R.; Salinas, C.; Pardo-Lozano, R.; Rabiner, E. A.; Farre, M.; Laruelle, M. *Synapse*, in press.
- Depoortère, R.; Dargazanli, G.; Estenne-Bouhtou, G.; Coste, A.; Lanneau, C.; Desvignes, C.; Poncelet, M.; Heaulme, M.; Santucci, V.; Decobert, M.; Cudennec, A.; Voltz, C.; Boulay, D.; Terranova, J. P.; Stemmelin, J.; Roger, P.; Marabout, B.; Sevrin, M.; Vigé, X.; Biton, B.; Steinberg, R.; Françon, D.; Alonso, R.; Avenet, P.; Oury-Donat, F.; Perrault, G.; Griebel, G.; George, P.; Soubrié, P.; Scatton, B. *Neuropsychopharmacology* **2005**, *30*, 1963.
- Mezler, M.; Hornberger, W.; Mueller, R.; Schmidt, M.; Amberg, W.; Braje, W.; Ochse, M.; Schoemaker, H.; Behl, B. *Mol. Pharmacol.* **2008**, *74*, 1705.
- Toyohara, J.; Ishiwata, K.; Sakata, M.; Wu, J.; Nishiyama, S.; Tsukada, H.; Hashimoto, K. *Nucl. Med. Biol.* **2011**, *38*, 517.
- Dargazanli, G.; Estenne-Bouhtou, G.; Magat, P.; Marabout, B.; Medaisko, F.; Roger, Pierre.; Sevrin, M.; Veronique, C. U.S. Patent 7,326,722 B2, 2008.
- Williams, J. B.; Mallorga, P. J.; Lemaire, W.; Williams, D. L.; Na, S.; Patel, S.; Conn, J. P.; Pettibone, D. J.; Austin, C.; Sur, C. *Anal. Biochem.* **2003**, *321*, 31.
- Wu, Z. L.; O'Kane, T. M.; Connors, T. J.; Marino, M. J.; Schaffhauser, H. *Brain Res.* **2008**, *1227*, 42.
- Mallorga, P. J.; Williams, J. B.; Jacobson, M.; Marques, R.; Chaudhary, A.; Conn, P. J.; Pettibone, D. J.; Sur, C. *Neuropharmacology* **2003**, *45*, 585.
- Herdon, H. J.; Roberts, J. C.; Coulton, S.; Porter, R. A. *Neuropharmacology* **2010**, *59*, 558.
- Jursky, F.; Tamura, S.; Tamura, A.; Mandiyan, S.; Nelson, H.; Nelson, N. J. *Exp. Biol.* **1994**, *196*, 283.
- Alberati-Giani, D.; Ceccarelli, S. M.; Pinard, E.; Stalder, H. W.O. Patent 2004072034, 2004.
- Waterhouse, R. N. *Mol. Imaging Biol.* **2003**, *5*, 376.
- Pike, V. W. *Trends Pharmacol. Sci.* **2009**, *30*, 431.
- Lear, J. L.; Ackermann, R. F.; Kameyama, M.; Kuhl, D. E. *J. Cereb. Blood Flow Metab.* **1982**, *2*, 179.
- Lear, J. L.; Navarro, D. J. *Nucl. Med.* **1987**, *28*, 481.
- Caulfield, W. L.; Collie, I. T.; Dickins, R. S.; Epemolu, O.; McGuire, R.; Hill, D. R.; McVey, G.; Morphy, J. R.; Rankovic, Z.; Sundaram, H. *J. Med. Chem.* **2001**, *44*, 2679.
- Perez-Medrano, A.; Nelson, D. W.; Carroll, W. A.; Kort, M. E.; Gregg, R. J.; Voight E. A.; Jarvis, M. F.; Kowaluk, E. A. W.O. Patent 2006086229, 2006.
- Zeng, Z.; O'Brien, J. A.; Lemaire, W.; O'Malley, S. S.; Miller, P. J.; Zhao, Z.; Wallace, M. A.; Raab, C.; Lindsley, C. W.; Sur, C.; Williams, D. L., Jr. *Nucl. Med. Biol.* **2008**, *35*, 315.